Real-time mapping of electronic structure with single-shot two-dimensional electronic spectroscopy

Elad Harel, Andrew F. Fidler, and Gregory S. Engel[1]

The James Franck Institute and Department of Chemistry, University of Chicago, Chicago, IL 60637

Edited* by Alexander Pines, University of California and Lawrence Berkeley National Laboratory, Berkeley, CA, and approved August 2, 2010 (received for review May 31, 2010)

Electronic structure and dynamics determine material properties and behavior. Important time scales for electronic dynamics range from attoseconds to milliseconds. Two-dimensional optical spectroscopy has proven an incisive tool to probe fast spatiotemporal electronic dynamics in complex multichromophoric systems. However, acquiring these spectra requires long point-by-point acquisitions that preclude observations on the millisecond and microsecond time scales. Here we demonstrate that imaging temporally encoded information within a homogeneous sample allows mapping of the evolution of the electronic Hamiltonian with femtosecond temporal resolution in a single-laser-shot, providing real-time maps of electronic coupling. This method, which we call GRadient-Assisted Photon Echo spectroscopy (GRAPE), eliminates phase errors deleterious to Fourier spectroscopies while reducing the acquisition time by orders of magnitude using only conventional optical components. In analogy to MRI in which magnetic field gradients are used to create spatial correlation maps, GRAPE spectroscopy takes advantage of a similar type of spatial encoding to construct electronic correlation maps. Unlike magnetic resonance, however, this spatial encoding of the nonlinear polarization along the excitation frequency axis of the two-dimensional spectrum results in no loss in signal while simultaneously reducing overall noise. Correlating the energy transfer events and electronic coupling occurring in tens of femtoseconds with slow dynamics on the subsecond time scale is fundamentally important in photobiology, solar energy research, nonlinear spectroscopy, and optoelectronic device characterization.

MRI | nonlinear response | photon echo | ultrafast phenomena | spatial encoding

Ultrafast optical spectroscopy can elucidate subpicosecond molecular dynamics, providing insight into vibrational and electronic structure and solute-solvent interactions in the IR and visible regions of the spectrum (1–6). Two-dimensional electronic spectroscopy directly probes correlations between electronic states providing detailed maps of energy transfer and coupling (7–10). However, as currently implemented two-dimensional spectroscopy provides no means by which to connect the initial dynamics in the first few hundred femtoseconds of electronic motion with slower dynamics associated with large structural changes. In a departure from the existing paradigm of point-by-point Fourier sampling, we map the multidimensional spectroscopic problem onto an imaging one by trading a temporal scan for a spatial dimension. This mapping permits the acquisition of the entire two-dimensional optical spectrum in a single-laser shot. Unlike other single-shot two-dimensional methods (11), which spatially encode the optical frequencies of the pulse and hence only provide static spectra, GRadient-Assisted Photon Echo (GRAPE) spectroscopy capitalizes on a temporal gradient imposed purely geometrically to encode time delays onto a spatial axis within the sample. The resultant spectrum provides an instantaneous snapshot of the electronic structure without losing the femtosecond time resolution needed to follow the electronic or vibrational dynamics of the system. Mercer et al. (12) have utilized a type of angular encoding to resolve the transition energies involved in a particular four-wave mixing pathway in a single-laser-shot. However, unlike photon echo spectroscopy, this method does not retain information encoded in the line shape such as the ability to distinguish inhomogeneous from homogeneous broadening. In addition, the angular encoding comes at the price of temporal smearing due to the finite crossing angles of the beams. GRAPE spectroscopy circumvents these limitations by harnessing the full power of two-dimensional photon echo spectroscopy with no temporal smearing and no loss in signal. Further, the method is easily implemented on existing spectrometers without linear delay stages, diffractive optics, pulse shapers, or phase stabilization.

The most notable difference between NMR and optical spectroscopy is the relative size of the sample to the wavelength. In the visible region of the spectrum the sample size is 100λ instead of $\lambda/100$ as in NMR. For nonlinear propagation, this large sample-to-wavelength ratio results in a background-free signal that emerges in a unique phase-matched direction. In NMR, the signal is emitted isotropically, and the detectors encompassing the sample must use phase cycling to isolate the desired coherence pathway. In the optical regime, the sample region illuminated by focused beams typically represents less than one part in 10^4 of the total sample area. Defocusing the light increases the number of molecules contributing to the signal but creates temporal broadening of the integrated signal due to the crossing angles of the beams (13). Previously, this effect has been regarded as an unwanted artifact and avoided by creating a tight focus at the sample in which the temporal gradient was smaller than the duration of the pulse (13). Here, we exploit this temporal gradient—and, in fact, magnify it—to generate a two-dimensional photon echo spectrum in a single laser shot with no loss in signal, despite the reduction in acquisition time by several orders of magnitude.

Two-dimensional electronic spectroscopy uses four identical femtosecond pulses to probe couplings between electronic states. This technique has successfully elucidated dynamics and microscopic interactions in semiconductor quantum wells (14), carbon nanotubes (15, 16), and photosynthetic light-harvesting complexes (10, 17) on femtosecond time scales. The first pulse, k_1, generates a one-quantum coherence in the sample that evolves for a time τ, before the second pulse, k_2, stores this evolved phase as a zero-quantum coherence, commonly referred to as a population. After a "waiting time," T, the third pulse, k_3, returns the system to a single-quantum coherence where an echo forms a time t_{echo} later. Frequency-resolved detection occurs by heterodyning the emitted signal with the local oscillator (LO) pulse, k_4. The third-order nonlinear polarization is then measured as a function of the two delay times, τ and T, for each emitted frequency. The two-dimensional spectrum generated for each

Author contributions: E.H. and G.S.E. designed research; E.H. and A.F.F. performed research; E.H. analyzed data; and E.H., A.F.F., and G.S.E. wrote the paper.

The authors declare no conflict of interest.

*This Direct Submission article had a prearranged editor.

[1]To whom correspondence should be addressed. E-mail: gsengel@uchicago.edu.

This article contains supporting information online at www.pnas.org/lookup/suppl/doi:10.1073/pnas.1007579107/-/DCSupplemental.

Downloaded by guest on November 28, 2021

waiting time by a double Fourier transform about the coherence and rephasing times, correlates the dipole oscillation during the initial period, τ, with that during the final period, t. Peaks on the diagonal therefore provide a measure of the "memory" of the system in which oscillating dipoles at a given frequency are correlated to one another at the same frequency at a later time, T. Cross-peaks provide information on electronic couplings between dipoles. Changes in the two-dimensional spectrum as a function of the waiting time reveal the dynamics of energy transfer among chromophores as well as interactions of chromophores with the bath. In the case of photon echo spectroscopy, inhomogeneous broadening along the direct t-domain is reduced to the homogeneous limit, making it particularly useful for systems with unresolvable linear spectra (10, 18).

All multidimensional optical Fourier-transform spectroscopies to date rely on point-by-point sampling schemes based on conventional two-dimensional NMR protocols. In each case, τ is systematically scanned for each population time. Due to the Fourier nature of the sampling, coherent multidimensional spectroscopy is highly susceptible to phase errors. Therefore, successful implementation of such spectroscopies, particularly in the visible region, requires either passive or active phase stabilization (19, 20).

In the two-dimensional GRAPE experiment introduced here, two pairs of 40 femtosecond pulses are generated using conventional beam splitters and mirrors, but rather than focusing to a point, the beams are focused to a line using a cylindrical lens (see *SI Text* for details of the optical setup). As with one-dimensional MRI, each point of this line (y-axis) along the sample contributes exactly one point to the overall signal. The variation in τ with space is created geometrically by tilting the wavefront of one beam relative to another by the relative angle, α between the focused lines using mirrors, resulting in a temporal gradient of slope $(\tan\alpha)/c$ along y (Fig. 1). For small angles, this gradient causes a delay across the unfocused beam diameter of a few hundred femtoseconds, which establishes the range of the τ values to be sampled. Similarly, all the pulses in the photon echo pulse sequence can be angled such that each position along the y-axis corresponds directly to a different indirect time-domain sequence, which in aggregate captures the whole two-dimensional experiment. Measuring the spatially resolved signal requires the use of an imaging spectrograph that spectrally resolves this distribution of points by projecting it onto a two-dimensional CCD camera.

To demonstrate the successful implementation of GRAPE, we measure the two-dimensional spectrum of a solvatochromic dye, IR 144 in methanol, for a range of waiting times. Because of the extensive studies on the ultrafast dynamics of dye molecules, IR 144 provides an important benchmark to compare the GRAPE method to the multiscan acquisition schemes that have been employed in two-dimensional optical spectroscopy in the condensed phase (7). The raw signal recorded by the CCD camera of IR 144 at ambient temperature is shown in Fig. 2*B*. The vertical stripes are a result of interference between the signal and the LO, k_4, for each position along the unfocused beam diameter. Fourier transformation along the horizontal frequency (or wavelength) axis leads to a τ-t plot that contains the spatially encoded photon echo. After appropriate apodization to remove the homodyne signal peak, a two-dimensional Fourier transformation generates the two-dimensional spectrum shown in Fig. 3 for $T = 0$ and $T =$ 100 fs. Separately recorded pump-probe measurements allow phasing of the two-dimensional spectrum to separate the real and imaginary contributions to the signal. Pump-probe fits show a nearly perfect fit to the projection of the real part of the two-dimensional spectrum in accordance with the projection-slice theorem. In agreement with previous reports on IR 144 (7), a small negative feature above the diagonal in the real part of the two-dimensional spectrum at $T = 0$ arises from four-level contributions that couple vibrationally excited states on the ground electronic surfaces. Due to fast relaxation resulting from strong coupling of the vibronic levels to the solvent, cross-peaks connecting different vibronic levels are poorly resolved at $T > 0$. The narrower line width in the antidiagonal direction compared to the homogeneous limit at $T = 0$ demonstrates the ability to reveal features otherwise inaccessible in inhomogeneously broadened systems. As the system loses memory of its initial absorption frequency at $T = 100$ fs the peak becomes rounder

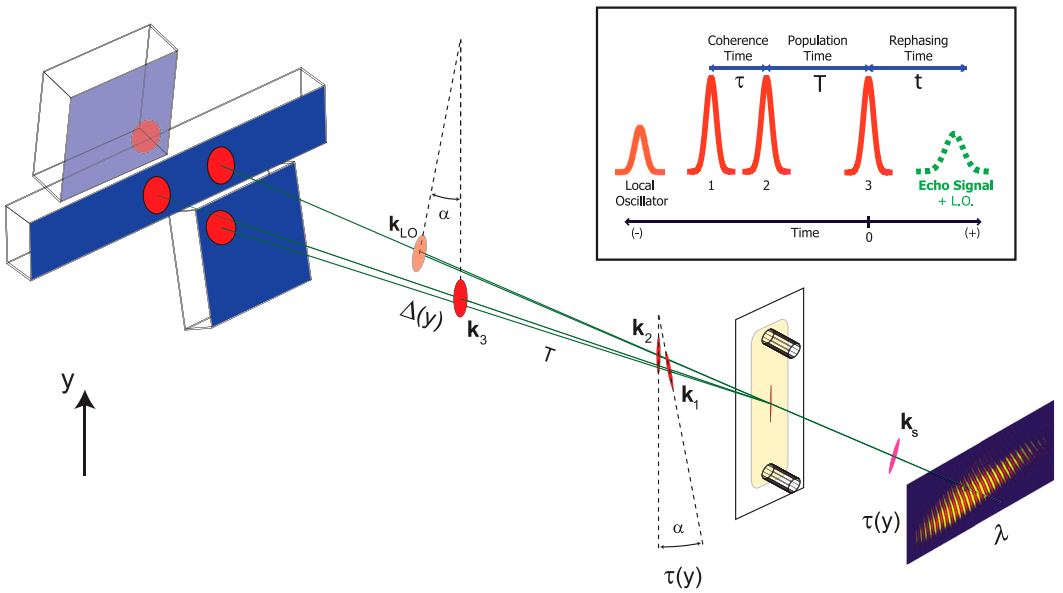

Fig. 1. Schematic of the GRAPE mirror assembly. Inset shows the pulse sequence used in two-dimensional photon echo spectroscopy. Two phase-matched pairs of pulses reflect from a wedged beamsplitter (see SOM) to form beams 1–4. Tilted wave fronts, created by reflections of a three-mirror assembly, are used to spatially encode the τ delay between pulses 1 and 2 while keeping pulses 2 and 3 at a constant delay time, T, across the sample. Beams 2 and 3 reflect off a single horizontal mirror and focus to parallel lines at the sample cell (cylindrical focusing lens not shown). Beam 1 is tilted at an angle, α, relative to beams 2 and 3, while the LO, beam 4, is tilted at an equal, but opposite angle to beam 1 to form the phase-matched geometry yielding signal in the rotating frame. The signal emanates in the direction of the LO for each point along the unfocused beam waist (y-direction) before being spectrally dispersed by a diffraction grating. The resultant two-dimensional image is recorded by a CCD camera.

Downloaded by guest on November 28, 2021

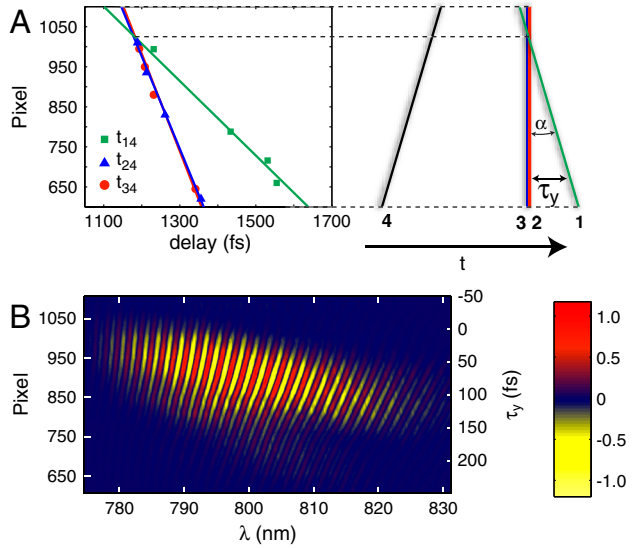

Fig. 2. Spatiotemporal Gradient. *A*. Temporal delay between pulse 1, 2, and 3 relative to the LO (4) as measured by spectral interferometry at $T = 0$. The slopes of t_{24} and t_{34} are kept identical to ensure a constant population time across the beam waist. The crossing point of t_{14} and t_{24} lines define the $\tau = 0$ point. A schematic of the corresponding pulse ordering along the beam waist is shown to the right. *B*. Raw signal as recorded on the CCD camera after background and scattering subtraction for $T = 0$ waiting time. The pixel axis is mapped with the $\tau(y)$ axis according to the interference patterns recorded in *A*.

and less resolved although a very small negative feature is still visible above the main diagonal. Finally, the maximum of the center peak in the real part of the spectrum lies below the main diagonal as a result of a Stokes shift due to solvent reorganization. We also observe a small negative feature below the diagonal

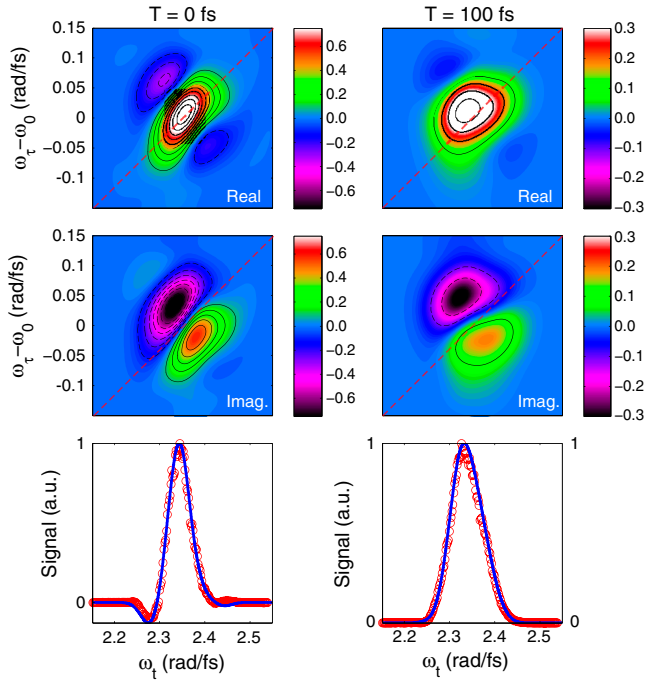

Fig. 3. Correlation Maps of Electronic Structure. Rephasing real (top) and imaginary (middle) two-dimensional spectra of 0.4 mM IR 144 in methanol at $T = 0$ and $T = 100$ fs. Contour lines are shown at 10% increments of the $T = 0$ real maximum signal. The data is phased (bottom) by matching the projection of the real part of the spectrum (blue curve) to spectrally resolved pump-probe measurements (red circles).

at $T = 0$, which arises from four-level contributions with negative dipole moment products (7), but until now have not been seen in experiment. Our ability to resolve this feature, which is attributed to solvent memory effects (vibrational narrowing) at very short times, results from the excellent signal-to-noise offered by GRAPE.

GRAPE offers several important advantages over multiscan approaches. Besides the decrease in acquisition time by a factor of about 500, a gain in signal-to-noise of the single-shot two-dimensional spectrum over the multiscan two-dimensional spectrum exists due to an actual reduction of the overall noise from the sample. In multiscan two-dimensional, the indirect dimension is susceptible to what is known in magnetic resonance as t_1 noise, so named because it primarily affects the indirect dimension (i.e., τ dimension in two-dimensional electronic photon echo spectroscopy) of two-dimensional spectroscopic experiments (21). As a result of fluctuations of the sample due to the environment and of instability in the experimental apparatus, t_1 noise may be transferred to the emitted signal. This noise is especially important to consider in Fourier experiments where phase errors cause distortion of the spectrum, primarily in the form of line broadening and reduced signal-to-noise. These phase errors may arise from nonuniform temporal sampling or fluctuations in laser power, temperature, alignment, index of refraction, or laser spectrum. A quantitative analysis of t_1 noise in GRAPE vs. multiscan acquisition schemes will be the subject of a future publication.

GRAPE is inherently phase stable because of its single-shot nature. All other two-dimensional methods to date must maintain phase stability of the pulses that generate the two-dimensional spectrum to reduce the t_1 noise, either passively (22) or actively (20), which can significantly increase the complexity of the experimental apparatus. The most pressing limitation of these multiscan methods is the stringent environmental stability needed throughout the duration of the sampling, specifically with regard to temperature, humidity, and vibration. GRAPE significantly relaxes the otherwise necessary environmental controls since all the simultaneously sampled points in the sample experience identical environments during any given laser pulse. Additionally, many important biological samples are either not viable for more than a few minutes at room temperature or demonstrate interesting dynamics on these time scales, precluding interrogation with multiscan acquisition schemes (23, 24). Combined with a significantly simplified optical setup, GRAPE has the potential to bring two-dimensional optical spectroscopy into the kind of widespread use currently enjoyed by multidimensional magnetic resonance spectroscopy. Unlike MRI, which partitions the sample using magnetic field gradients, GRAPE spectroscopy achieves no loss in signal compared to multiscan approaches. The orders of magnitude reduction in acquisition time will permit practical implementation of three-dimensional optical spectroscopy to resolve obscured spectral features as well as real-time monitoring of chemical dynamics with fast imaging detectors.

Methods

See *SI Text*.

Optical Apparatus. A single 6 mm diameter pulse was generated using a Coherent Legend Elite USP-HE regenerative amplifier (40 fs, 5 kHz, 800 nm) seeded by a Coherent Micra titanium sapphire oscillator (81 MHz, 800 nm). The output of the regenerative amplifier is split by a 50:50 beam splitter, and the delay between the two beams, corresponding to the waiting time, T, is controlled with a motorized translation stage (Aerotech, Inc.). Each beam is further split into a pair by the use of front and back Fresnel reflections from a 3 mm thick uncoated glass wedge of half a degree. The input angles to the wedged optic are adjusted such that the back reflection of the 1,2 pair is parallel to the front reflection of the 3,4 pair. Assuming small angles, this arrangement results in identical relative angles between beams 1 and 2 and between beams 3 and 4, which are formed by the remaining front and back reflections. For a wedge of angle, β, the relative angle

Downloaded by guest on November 28, 2021

between the 1, 2 and 3, 4 beams is given by $\gamma = 2n_g\,\beta$, where n_g is the index of refraction of the glass. See *SI Text* for details of the optical setup.

The four resulting beams are then incident on the GRAPE mirror assembly to form the distorted boxcar geometry. The LO (i.e., beam 4), is attenuated by utilizing the front Fresnel reflection from an uncoated optical flat followed by neutral density placed after the mirror assembly, resulting in a total attenuation of approximately three orders of magnitude. The mirrors in the GRAPE assembly are oriented such that the vertical position of the four beams overlaps at the sample to generate the required tilted wave fronts that spatially encode the temporal delays across the sample and permit acquisition of the echo signal in the rotating frame. A 250 mm focal length cylindrical lens focuses the four beams in the horizontal direction onto a vertical line in the sample. At the sample, the pulse energy is 50 nJ per pulse, resulting in an energy flux of 14 $\mu J/cm^2$, which is comparable to other multiscan setups that focus to a spot. Two spherical mirrors with respective focal lengths 50 cm and 25 cm act to image the emitted line of signal at the sample to a 25 μm slit at the interferometer (Andor Technology). A spatial filter is placed at the focus of the first spherical mirror (SM1) after the sample, which isolates only the photon echo signal and LO. The interferometer spectrally resolves the resulting heterodyned with a 1,200 lines/mm grating on a $2{,}048 \times 2{,}048$ CCD detector (Andor Technology). The resulting interference pattern allows for the determination of the phase and magnitude of the third-order rephasing signal.

Sample. The laser dye IR 144 (Exciton) was dissolved in methanol to create a 0.4 mM solution with an optical density of approximately 0.3 at 800 nm in a 200 μm fused quartz flow cell (Starna). Solutions were prepared immediately prior to the experiment to avoid sample degradation. All measurements were taken at the ambient temperature of 21 °C.

Pulse Timings. The timings between pulses were determined using spectral interferometry as described by Joffre and coworkers (25) A scattering element was placed at the sample position, and the timings of beams 1, 2, and 3 were separately measured with respect to beam 4. The timing of beam 1 with respect to beam 2 was set to create a temporal gradient from approximately −200 fs to 400 fs across the beam waist, corresponding to approximately 0.6 fs/pixel at the detector. Beam 4 was attenuated to avoid unwanted pump-probe signals and delayed by $\Delta(y)$ such that the center of the wave front arrives approximately 1.3 ps before beam 3. Because of the orientation of the beam 1 and beam 4 mirrors, the temporal gradient of beam 4 relative to beam 3 is opposite in sign to the temporal gradient between beam 1 and 2, $\partial\tau(y)/\partial y = -\partial\Delta(y)/\partial y$. Since the signal in a photon echo experiment comes out a time, τ after beam 3 (neglecting the photon echo peak shift), the time between beam 4 and the signal is constant at all positions in the sample. However, due to the delays caused by the back reflection in the wedged beam splitter, the position of the mirrors in the GRAPE assembly along the propagation direction are not exactly in the same vertical plane, causing a slight tilt of the echo relative to the LO.

Data Analysis. Our data analysis uses a modified procedure of that used for multiscan two-dimensional spectroscopy as described in detail by Brixner et al. (19) The scatter-subtracted heterodyne-detected signal is Fourier transformed in the wavelength dimension to create a time vs. λ^{-1} dataset containing the homodyne and photon echo. The scattering data is used to convert pixels in the y direction into τ values, and a Fourier interpolation algorithm is used to convert the wavelength dimension to evenly spaced time points. A windowing function is then applied to isolate the photon echo signal. A cut through the echo shows oscillations corresponding to phase evolution of the signal during the coherence time τ as expected. Due to the rotating frame detection scheme, only the difference frequencies in the oscillations are detected, rather than the optical frequency itself. Finally, a two-dimensional Fourier transform is applied to the entire τ-t dataset, resulting in a two-dimensional spectrum for each population time. The absolute phase of the spectra was then determined by fitting to a separately recorded pump-probe signal.

ACKNOWLEDGMENTS. The authors thank the NSF MRSEC (DMR 08-00254), AFOSR (FA9550-09-1-0117) and the Searle Foundation for Support. E.H. would like to acknowledge support from the National Science Foundation Grant DMR-0844115 and the Institute for Complex Adaptive Matter Branches Cost-Sharing Fund.

1. Maroncelli M, Macinnis J, Fleming GR (1989) Polar-solvent dynamics and electron-transfer reactions. *Science* 243:1674–1681.
2. Jimenez R, Fleming GR, Kumar PV, Maroncelli M (1994) Femtosecond solvation dynamics of water. *Nature* 369:471–473.
3. Hamm P, Lim M, DeGrado WF, Hochstrasser RM (1999) The two-dimensional IR nonlinear spectroscopy of a cyclic penta-peptide in relation to its three-dimensional structure. *Proc Nat'l Acad Sci USA* 96:2036–2041.
4. Fecko CJ, Eaves JD, Loparo JJ, Tokmakoff A, Geissler PL (2003) Ultrafast hydrogen-bond dynamics in the infrared spectroscopy of water. *Science* 301:1698–1702.
5. Cowan ML, et al. (2005) Ultrafast memory loss and energy redistribution in the hydrogen bond network of liquid H2O. *Nature* 434:199–202.
6. Mukamel S (1995) *Principles of nonlinear optical spectroscopy* (Oxford University Press, New York, Oxford).
7. Hybl JD, Ferro AA, Jonas DM (2001) Two-dimensional Fourier transform electronic spectroscopy. *J Chem Phys* 115:6606–6622.
8. Scheurer C, Mukamel S (2001) Design strategies for pulse sequences in multidimensional optical spectroscopies. *J Chem Phys* 115:4989–5004.
9. Cowan ML, Ogilvie JP, Miller RJD (2004) Two-dimensional spectroscopy using diffractive optics based phased-locked photon echoes. *Chemical Phys Lett* 386:184–189.
10. Brixner T, et al. (2005) Two-dimensional spectroscopy of electronic couplings in photosynthesis. *Nature* 434:625–628.
11. DeCamp MF, DeFlores LP, Jones KC, Tokmakoff A (2007) Single-shot two-dimensional infrared spectroscopy. *Opt Express* 15:233–241.
12. Mercer IP, et al. (2009) Instantaneous mapping of coherently coupled electronic transitions and energy transfers in a photosynthetic complex using angle-resolved coherent optical wave-mixing. *Phys Rev Lett* 102:057402.
13. Yetzbacher MK, Belabas N, Kitney KA, Jonas DM (2007) Propagation, beam geometry, and detection distortions of peak shapes in two-dimensional Fourier transform spectra. *J Chem Phys* 126:044511.
14. Stone KW, et al. (2009) Two-quantum 2D ft electronic spectroscopy of biexcitons in gaas quantum wells. *Science* 324:1169–1173.
15. Milota F, et al. (2009) Excitonic couplings and interband energy transfer in a double-wall molecular aggregate imaged by coherent two-dimensional electronic spectroscopy. *J Chem Phys* 131:054510.
16. Nemeth A, et al. (2009) Tracing exciton dynamics in molecular nanotubes with 2D electronic spectroscopy. *Chemical Phys Lett* 469:130–134.
17. Engel GS, et al. (2007) Evidence for wavelike energy transfer through quantum coherence in photosynthetic systems. *Nature* 446:782–786.
18. Cho MH, Fleming GR (2005) The integrated photon echo and solvation dynamics. Ii. Peak shifts and two-dimensional photon echo of a coupled chromophore system. *J Chem Phys* 123:114506.
19. Brixner T, Mancal T, Stiopkin IV, Fleming GR (2004) Phase-stabilized two-dimensional electronic spectroscopy. *J Chem Phys* 121:4221–4236.
20. Volkov V, Schanz R, Hamm P (2005) Active phase stabilization in Fourier-transform two-dimensional infrared spectroscopy. *Opt Lett* 30:2010–2012.
21. Mehlkopf AF, Korbee D, Tiggelman TA, Freeman R (1984) Sources of t1 noise in two-dimensional NMR. *J Magn Reson* 58:315–323.
22. Ding F, Mukherjee P, Zanni MT (2006) Passively correcting phase drift in two-dimensional infrared spectroscopy. *Opt Lett* 31:2918–2920.
23. Strasfeld DB, Shim SH, Zanni MT (2009) New advances in mid-IR pulse shaping and its application to 2D IR spectroscopy and ground-state coherent control. *Adv Chem Phys* 141:1–28.
24. Shim SH, Strasfeld DB, Ling YL, Zanni MT (2007) Automated 2D IR spectroscopy using a mid-IR pulse shaper and application of this technology to the human islet amyloid polypeptide. *Proc Nat'l Acad Sci USA* 104:14197–14202.
25. Dorrer C, Belabas N, Likforman JP, Joffre M (2000) Spectral resolution and sampling issues in Fourier-transform spectral interferometry. *J Opt Soc Am B* 17:1795–1802.

Downloaded by guest on November 28, 2021